Acute Pancreatitis Signals Activation of Apoptosis-Associated and Survival Genes in Mice

GUILLERMO GOMEZ,* HEUNG-MAN LEE,* QIN HE,* ELLA W. ENGLANDER,* TATSUO UCHIDA,† AND GEORGE H. GREELEY, JR.*,[1]

Department of Surgery and †Office of Biostatistics, The University of Texas Medical Branch, Galveston, Texas 77555

In experimental models of acute pancreatitis (AP), acinar cell death occurs by both necrosis and programmed cell death or apoptosis. Apoptosis is an active form of cell death associated with a tightly regulated expression of gene products that are either pro- or antiapoptotic. The aim of this study was to characterize pancreatic mRNA levels by Northern blotting analysis of apoptosis-associated genes used during the course of cerulein-induced AP in mice. Histone H3 mRNA levels were also examined as an indicator of cell proliferation. Acinar cell apoptosis was confirmed histologically. The findings show that AP modifies pancreatic mRNA levels of both pro- and antiapoptotic genes simultaneously. Pancreatic bcl_{XL}, bax, and p53 mRNA levels increased significantly in a temporal fashion during induction of AP. Pancreatic bcl-2 mRNA levels were unchanged during AP. Pancreatic mRNA levels of insulin-like growth factor-1 (IGF-1), a mitogen and cell survival factor, and its receptor (IGF-1R) also increased in a temporal fashion during induction of AP. In summary, this study indicates that acinar cell death during cerulein-induced AP in mice can occur by the apoptotic pathway. Since factors promoting and antagonistic for cell survival are activated simultaneously, regulation of acinar cell survival appears complex and dynamic during AP.

[Exp Biol Med Vol. 226(7):692–700, 2001]

Key words: apoptosis; gene products; acute pancreatitis; Western blotting; Northern blotting

In man, acute pancreatitis (AP) is a severe disease with a significant morbidity and mortality (1). In order to better understand the underlying cellular mechanisms of AP in humans, several experimental animal models of AP have been developed. These models include a choline-deficient and ethionine-supplemented diet, obstruction of the pancreatic duct, and infusion of supramaximal doses of cholecystokinin or its longer acting analogue, cerulein (2–8). Cerulein-induced pancreatitis results in a nonlethal edematous pancreatitis and shows many of the features of human pancreatitis, including elevated systemic amylase levels, pancreatic edema, inflammation, and cell death (2, 9). In pancreatitis, acinar cell death occurs by both necrosis and programmed cell death or apoptosis (10–15). Apoptosis is an active process of cell death dependent upon induction of specific genes (16–18). In rodents, AP-induced acinar cell death is accompanied by pancreatic recovery, including an increased mitotic activity of acinar cells (7, 8, 19, 20). Therefore, expression of genes involved in stimulation of acinar cell proliferation and pancreatic recovery is expected to increase. Cell death by the apoptotic pathway is also expected to occur during pancreatic remodeling to remove the surfeit of acinar cells (13, 16, 21).

The purpose of the present study, therefore, was to characterize mRNA levels of apoptosis-associated genes (bcl_{XL}, bcl-2, bax, p53, and IGF-1) during cerulein-induced AP in mice. In addition, the mRNA levels of a proliferation and cell survival factor, insulin-like growth factor-1 (IGF-1) and its receptor, the IGF-1 receptor (IGF-1R), during cerulein-induced AP were characterized. Pancreatic bax protein levels during AP were also examined by Western blotting analysis, and acinar cell production of bax protein was confirmed by immunohistochemical localization. Histone H3 mRNA levels were also used as an indicator of cell proliferation (22).

Numerous studies have shown that IGF-1 is a powerful cell survival factor (23–25). In neuronal cells (26), serum-deprived COS cells (27), atretic ovarian follicles (28), and in mammary gland involution (29), IGF-1 can block apop-

This work was supported by grants from the National Institutes of Health (RO1 DK15241 and PO1 DK 35608).

[1] To whom requests for reprints should be addressed at Department of Surgery, The University of Texas Medical Branch, 301 University Boulevard, Galveston, TX 77555-0725. E-mail: ggreeley@utmb.edu

Received October 24, 2000.
Accepted February 15, 2001.

0037-9727/01/2267-0692$15.00

tosis. IGF-1R may also have a role in controlling cell survival. For instance, the magnitude of apoptosis in tumor cells is inhibited when IGF-1R expression is increased (30, 31).

We found that pancreatic mRNA levels of pro- and anti-apoptotic genes increased significantly 8 to 48 hr after induction of AP. Pancreatic levels of bax protein also increased significantly during AP. Since expression of factors promoting and antagonistic for cell survival is activated concurrently, regulation of acinar cell survival during AP appears complex and dynamic.

Materials and Methods

Animals. AP was induced in female Swiss-Webster mice (22–26 g) by administration of supramaximal doses of cerulein (50 μg/kg, intraperitoneally, seven hourly injections, including 0 h for 6 h). Cerulein was purchased from Bachem California (Torrance, CA). Mice were sacrificed at selected intervals and the pancreas was removed immediately for preparation of pancreatic RNA and protein extracts, or for histological examination of acinar cell apoptosis. Trunk blood samples were collected at sacrifice and serum was prepared by centrifugation.

Histological Examination of Apoptosis and Immunohistochemical Localization of Bax. Acinar cell apoptosis was visualized by light microscopic examination of hematoxylin and eosin-(H&E) stained, paraffin-embedded pancreatic tissue sections (2–3 μm). Acinar cells were considered apoptotic when they showed condensed and/or fragmented nuclei.

Immunohistochemical localization of pancreatic bax was done on 4-μm sections of formalin-fixed and paraffin-embedded tissues using a rabbit anti-human polyclonal antibody, a goat anti-rabbit secondary antibody (Santa Cruz Biotechnology, Santa Cruz, CA), and a VECTASTAIN Elite ABC kit (Vector Laboratories, Burlingame, CA). Endogenous peroxidase activity was quenched with 3% H_2O_2 in methanol for 15 min followed by a rinse and incubation in PBS for 5 min. After incubation in dilute (~2%) nonimmune goat serum, slides were incubated with the anti-bax antibody (1:200, prepared in diluted goat serum) overnight at 4°C, followed by a PBS rinse and incubation with a rabbit biotinylated secondary antibody for 30 min and another PBS rinse. Slides were then incubated in the ABC reagent for 40 min, rinsed, and developed using the substrate diaminobenzidine solution for 5 min. Sections were rinsed three times for 10 min in distilled water and were counterstained with hematoxylin, dehydrated, and then coverslipped for light microscopy.

Preparation of RNA and Northern Blotting Analysis. Our procedure for preparation of pancreatic RNA is described in detail due to the difficulty in preparing intact pancreatic RNA. The entire pancreas was removed immediately and homogenized in 5 ml of 5 M guanidine thiocyanate containing 50 mM Tris HCl, 1% N-lauroyl sarcosine, 10 mM EDTA, pH 7.5, with 1% β-mercaptoethanol. Homogenates were allowed to settle briefly on ice and were then precipitated (24–48 hr) at 4°C by adding 7× volume ice-cold (~35 ml) 5 M LiCl. RNA precipitates were then pelleted and resuspended in 5 ml of 5 M guanidine thiocyanate containing 1% β-mercaptoethanol followed by one-tenth volume (~500 μl) 2 M sodium acetate, pH 4. RNA was then extracted twice by addition of 1.5 ml of chloroform plus 4 ml of phenol:chloroform mixture (5:1, pH 4.7, Sigma-Aldrich), and then a 2-ml chloroform wash. RNA was precipitated with an equal volume of isopropanol at −20°C overnight. RNA pellets were rinsed with 75% ethanol and then resuspended promptly in 4 ml of diethyl pyrocarbonate (DEPC)-treated water. RNA was extracted again by adding one-tenth volume sodium acetate (~400 μl), 1 ml of chloroform, and 2 ml of phenol:chloroform mixture (5:1, pH 4.7). The top phase was transferred and rinsed with 2 ml of chloroform. RNA was precipitated by addition of ethanol (2.5 volume) and incubated overnight at −20°C or for 2 hr at −70°C. RNA pellets were transferred to microcentrifuge tubes and rinsed with 75% ethanol followed by a 100% ethanol rinse. For preparation of polyadenylated $(A)^+$ RNA [poly$(A)^+$], samples were suspended in DEPC-treated water.

Poly$(A)^+$ mRNA was prepared by incubating (~1 mg) RNA samples with 100 mg of oligo(dt) cellulose (Stratagene, San Diego, CA) overnight in a high salt binding buffer (10 mM TRIS-HCl , pH 7.5, 1 mM EDTA, pH 8.0, 0.1% SDS, and 0.5 M NaCl). Samples were then washed with high salt buffer and then with (1.5–2 ml) low salt binding buffer (10 mM TRIS-HCl, 1 mM EDTA, 0.2% SDS, and 0.1 M NaCl) and eluted with salt-free buffer (10 mM TRIS-HCl, 1 mM EDTA, and 0.05% SDS). Poly$(A)^+$ mRNA samples were denatured twice (i.e., separated by vortexing) in a formamide/formaldehyde-containing gel loading buffer for 5 min at 65°C before separation by electrophoresis (10 μg) on a 1.0% denaturing agarose gel containing 1× MOPS [20 mM 3-(*N*-morpholino) propanesulfonic acid (pH 7.0) containing 8 mM sodium acetate, 1 mM EDTA (pH 8.0), and 5% formaldehyde. Transcript sizes were determined by comparison with migration of an RNA ladder (Ambion, Austin, TX, Millennium marker, 0.5–9 kb). The poly$(A)^+$ mRNA specimens and ladder were blotted onto nylon filters (brightstar nylon membranes, Ambion) and were cross-linked by means of an UV cross linker.

Membranes were then pre-hybridized and hybridized according to the instructions supplied with Strip-EZ RNA kits (Ambion). Multiple membranes were used in these analyses. After pre-hybridization for 16 to 24 hr, membranes were then hybridized with alpha ^{32}P-UTP-radiolabeled cRNA riboprobes (5–6 × 10^6 cpm/ml) overnight at 65°C. Membranes were washed three times for 5 to 10 min each at room temperature in 2× SSC-0.1% SDS, followed by three 30-min washes in 0.2× SSC-0.1% SDS at 65°C, and then depending upon the probe, this was followed by a high stringency wash for 30 min at 68°C (temperature varies with probe) in 0.1× SSC-0.1% SDS.

Membranes were exposed to Kodak Biomax MR film at −80°C between intensifying screens. Signal intensity on x-ray films was quantified by densitometric analysis (LYNX Molecular Biology Workstation by Image Recognition Systems, an Applied Imaging Company, Cheshire, UK).

To ensure the accuracy of the changes in mRNA abundance and equal loading and transfer of RNA, mRNA levels were normalized to pancreatic chymotrypsin mRNA abundance. mRNA levels of pancreatic chymotrypsin do not change during AP (see "Results").

Probes were obtained as follows: a mouse bax cDNA in pBluescript SK vector was obtained from S.J. Korsmeyer (32); the rat IGF-1 cDNA containing a 404-bp EcoR1 restriction fragment-1 (IGF-1) was provided by C.T. Roberts, Jr. (33); rat bcl-2 cDNA was obtained from J.C. Reed (34); rat bcl_{XL} cDNA was obtained from C.B. Thompson (35); rat histone H3 cRNA in pGEM3 vector was obtained from (22) and, the rat IGF-1R cDNA containing a 310-bp Eco R1 restriction fragment was obtained from D. LeRoith (36). Plasmids for rat p53 and chymotrypsin were purchased from ATCC (Rockville, MD).

Western Blotting Analysis. Pancreatic protein extracts were prepared by homogenizing pancreatic tissue pieces (<100 mg) immediately upon collection in RIPA buffer (50 mM TRIS-HCl, pH 7.5, with 150 mM NaCl, 0.1% SDS, 1.0% Nonidet P-40, 0.5% sodium deoxycholate, 0.1 mg/ml of phenylmethylsulfonyl fluoride, and 0.2 unit/ml aprotinin and this was supplemented with a freshly prepared protease inhibitor cocktail [Sigma, St. Louis, MO]). Supernatant protein concentrations were measured using the Bradford reagent (Bio-Rad, Hercules, CA). Aliquots of pancreatic extracts (30 μg of protein diluted with Laemmli loading buffer [Bio-Rad]) were then boiled for 5 min and then electrophoresed on a 10% SDS polyacrylamide gel, transferred onto polyvinylidene difluoride membrane, and probed with an antibody for bax (Santa Cruz Biotechnology). Signals were detected using enhanced chemiluminescence.

Serum Amylase Measurements. Serum amylase levels were determined using the Phadebas Amylase Test (Pharmacia and Upjohn Diagnostics AB, Uppsala, Sweden).

Statistical Analysis. Data were analyzed using the Kruskal-Wallis test with $\alpha = 0.05$. Fisher's least significant difference procedure on rank transformed data was used for multiple comparisons with $\alpha = 0.005$ for comparison wise error rate.

Results

Cerulein-induction of AP was verified by an acute elevation in serum amylase levels (Fig. 1).

Light microscopic examination of H&E-stained pancreatic sections showed acinar cell apoptosis after induction of cerulein-induced AP (Fig. 2). Ninety-six hours after induction of AP, a majority of the pancreatic damage is reversed and the pancreas has regenerated. Pancreatic islets

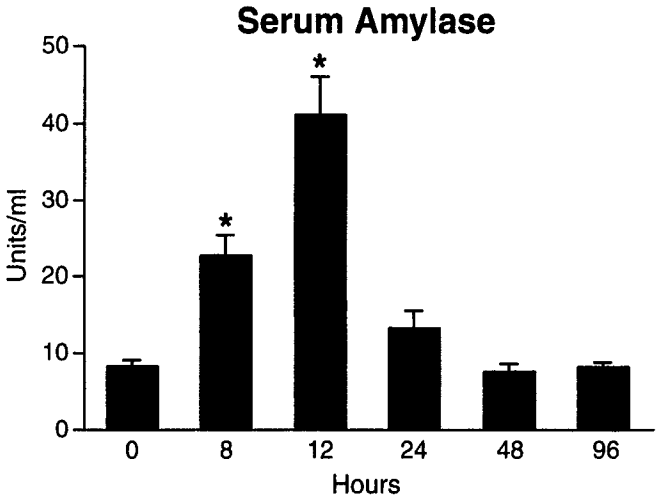

Figure 1. Serum amylase levels in mice with cerulein-induced AP. Mice were given seven hourly intraperitoneal injections of cerulein (50 μg/kg body wt).

were unaffected (data not shown). Examination of H&E-stained sections showed the greatest occurrence of acinar cell apoptosis 48 hr after induction of AP (Table I).

Northern blotting analysis of pancreatic poly(A)$^+$ mRNA extracts showed that pancreatic mRNA levels of pro- and anti-apoptotic genes increased significantly ($P < 0.005$ versus control levels) to peak levels 8 to 48 hr after cerulein-induction of AP in mice. mRNA levels then dropped precipitously 96 hr after induction of AP; however they remained elevated when compared with control levels.

Pancreatic mRNA levels of bcl-2, an anti-apoptotic gene, did not change during AP (data not shown). However, pancreatic bcl_{XL} mRNA levels increased approximately 120-fold 8 and 12 hr ($P < 0.005$) after induction of AP, and then decreased significantly 24, 48, and 96 hr after induction of AP (Fig. 3). Fourteen days after induction of AP, pancreatic bcl_{XL} mRNA levels did not differ significantly from control levels. Pancreatic p53 mRNA levels increased significantly, in a stepwise fashion, 8 to 24 hr after induction of AP (Fig. 4). Twenty-four to 48 hr after induction of AP, pancreatic p53 mRNA levels were approximately 35-fold greater than control levels. Pancreatic p53 mRNA levels remained significantly elevated 96 hr after induction of AP. Fourteen days after induction of AP, pancreatic p53 mRNA levels did not differ significantly from control levels.

Pancreatic bax mRNA levels increased approximately 7- and 13-fold, 12 and 24 hr after induction of AP and remained at a near-peak level 48 hr after induction of AP (Fig. 5). Pancreatic bax mRNA levels then declined significantly 96 hr after induction of AP. Fourteen days after induction of AP, pancreatic bax mRNA levels did not differ significantly from control expression levels. Western blotting analysis showed that pancreatic bax protein levels increased significantly to a peak level 48 hr after induction of AP. Bax protein levels then declined, although they remained significantly elevated 96 hr and 14 d after induction

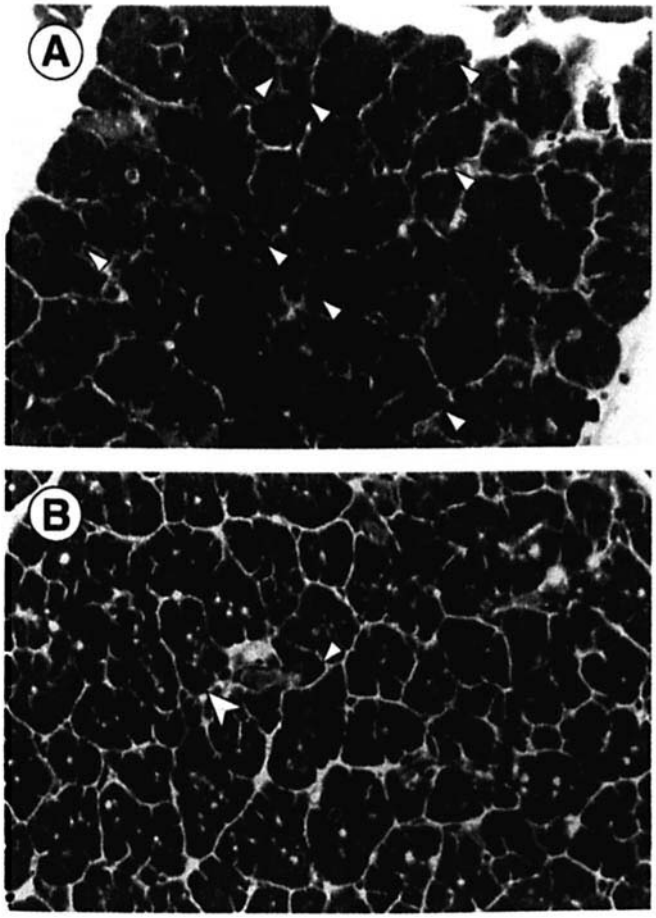

Figure 2. Representative photomicrographs showing pancreatic histology in mice with cerulein-induced AP. (A) Twelve hours after the beginning of cerulein injections. Pancreatic sections were stained with H&E. Notice the strong intracellular edema and abundant apoptotic acinar cells. Many acinar cell nuclei are condensed, fragmented, and dispersed in the condensed cytoplasm. Some apoptotic cells (condensed and fragmented nuclei) are identified by white arrowheads, 400×. (B) Ninety-six hours after the beginning of cerulein injections. Notice the relative paucity of apoptotic cells. A mitotic acinar cell is identified by the large white arrowhead and an apoptotic cell is identified by the small white arrowhead.

of AP when compared with control levels (Fig. 6). In agreement with Western blotting findings, bax immunostaining was observed in the pancreas of control mice (Fig. 7). Immunostaining showed abundant localization of bax protein in acinar cells of mice with AP. Bax immunostaining was detected in the cytoplasm and nuclei of apoptotic acinar

Table I. Measurement of Apoptosis at Selected Intervals During Caerulein-Induced AP in Mice

Group	Apoptosis (% of acinar cell counted)
Control	0.4 ± 0.2
8 hr after induction of AP	5.3 ± 2.6[a]
48 hr after induction of AP	10.7 ± 3.1[a]
14 days after induction of AP	1.5 ± 0.8

Note. Using H&E-stained sections, 1000 acinar cells in three mice/group were counted. Acinar cells were considered apoptotic when they showed condensed and/or fragmented nuclei.
[a] $P < 0.05$ versus control mice.

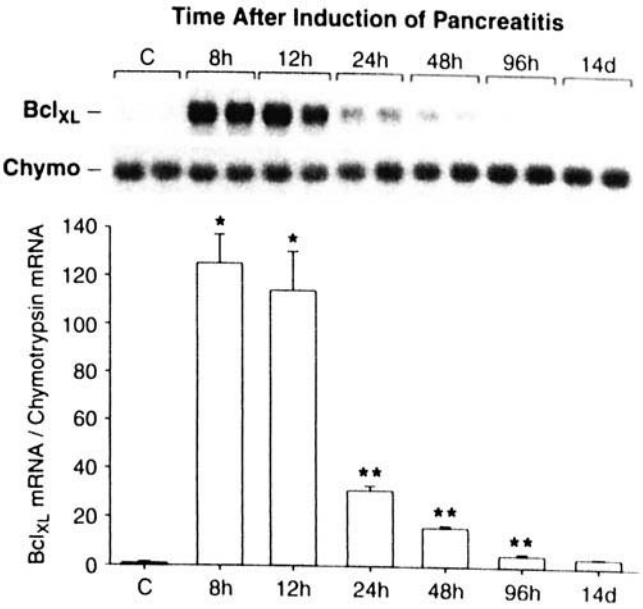

Figure 3. Northern blotting analysis of pancreatic bcl$_{XL}$ mRNA levels at different times after induction of AP by cerulein in mice. In this and subsequent figures, pancreatic mRNA levels of various apoptosis-associated genes are shown as a Northern blot and as a bar graph. For the Northern blotting analysis, 10 μg of pancreatic poly(A)$^+$ mRNA was electrophoresed in a formaldehyde-denaturing gel, transferred onto a nylon membrane, and hybridized with a ^{32}P-labeled cRNA probe. Membranes are also hybridized with a rat chymotrypsin cRNA probe (chymo) to correct for loading and transfer differences. Pancreatic chymotrypsin mRNA levels do not change in AP ($P > 0.05$). Only two lanes of each group are shown, although $n = 4$ pools of pancreatic poly(A)$^+$ mRNA prepared from different mice. * = $P < 0.005$ versus controls (C); ** = $P < 0.005$ versus controls and earlier groups. The bar graph shows the ratio of bcl$_{XL}$ mRNA over chymotrypsin mRNA densitometric readings for Northern blots. The mean ± SEM is shown.

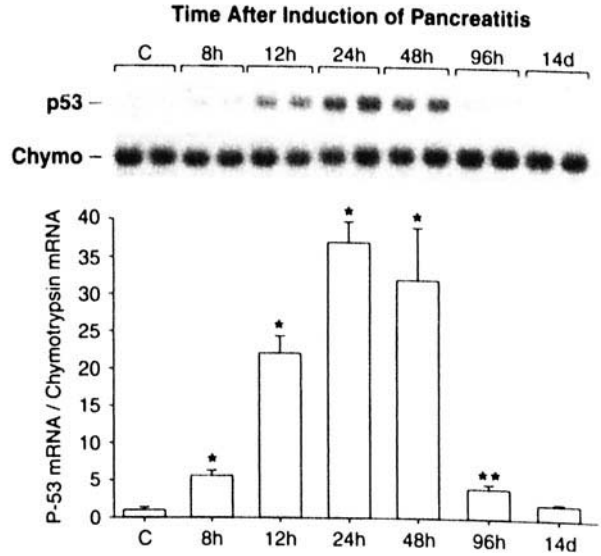

Figure 4. Northern blotting analysis of pancreatic p53 mRNA levels at different times after induction of AP in mice. * = $P < 0.005$ versus controls (C); ** = $P < 0.005$ versus controls and earlier groups.

cells. During AP, not all acinar cytoplasm and nuclei were immunostained for bax. Acinar cells also showed nuclei, but not the cytoplasm, immunostained for bax. A maximal bax immunostaining was observed 48 hr after induction of AP.

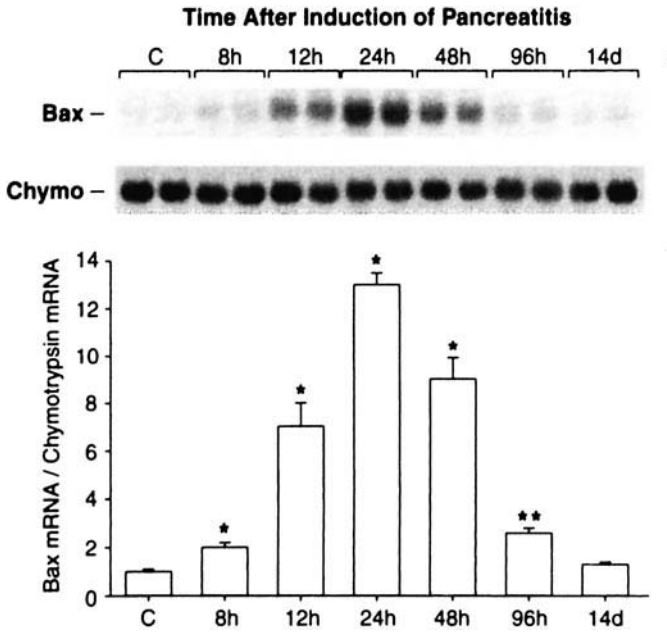

Figure 5. Northern blotting analysis of pancreatic bax mRNA levels at different times after induction of AP in mice. * = $P < 0.005$ versus controls (C); ** = $P < 0.005$ versus controls and earlier groups.

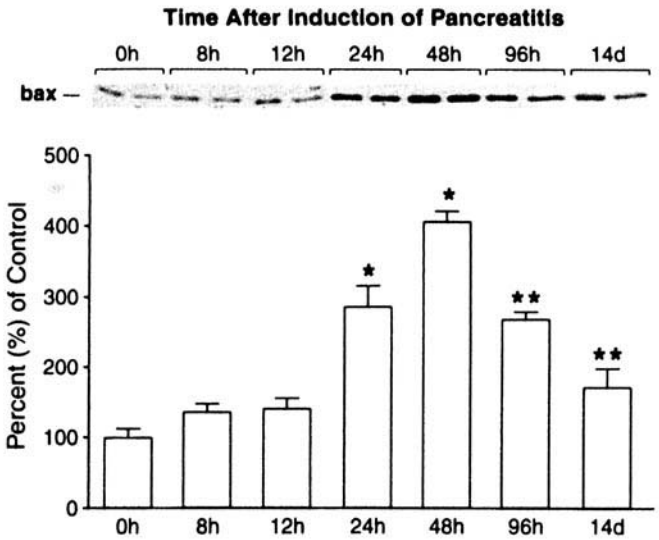

Figure 6. Western blotting analysis of pancreatic bax protein levels at different times after induction of AP in mice. Protein was extracted from pancreatic specimens harvested after induction of AP in mice. The blot was probed with a bax antiserum. n = 3 to 4 mice/time period. * = $P < 0.005$ versus controls (C); ** = $P < 0.005$ versus controls and earlier groups.

Pancreatic IGF-1 mRNA levels increased significantly 24 and 48 hr after induction of AP (Fig. 8). IGF-1 mRNA levels then declined precipitously 96 hr after induction of AP, although levels remained significantly elevated when compared with control levels. Fourteen days after induction of AP, pancreatic IGF-1 mRNA levels did not differ significantly when compared with control levels. Pancreatic IGF-1R mRNA levels increased significantly 8 to 48 hr after induction of AP and then declined at 96 hr and 14 days after induction of AP (Fig. 9). Pancreatic IGF-1R mRNA levels at 96 hr and 14 days did not differ significantly when compared with control levels.

Pancreatic histone H3 mRNA levels increased approximately 17- to 30-fold 8 to 12 hr after induction of AP and then remained significantly elevated 24 to 96 hr after induction of AP (Fig. 10). Fourteen days after induction of AP, pancreatic histone H3 mRNA levels did not differ significantly when compared with control levels.

Discussion

The findings of the present study demonstrate that pancreatic mRNA levels of several apoptosis–associated genes and IGF-1 are acutely upregulated in a temporal fashion during cerulein-induced AP in mice. Pancreatic mRNA levels of anti- and pro-apoptotic genes achieve peak values 8 to 48 hr after induction of AP. Remarkably, pancreatic mRNA levels of bcl_{XL}, an anti-apoptotic gene (37, 38), increase approximately 130-fold within 8 hr after the initial administration of cerulein. Pancreatic mRNA levels of two other apoptosis-associated genes, bax and p53, are also increased maximally within 12 to 48 hr after induction of AP. In the cases of bax and p53, these genes are pro-apoptotic (37, 39, 40). Additionally, pancreatic mRNA levels of bcl-2, an antiapoptotic gene, did not change during AP (data not shown). Pancreatic mRNA levels of IGF-1, which has a cell survival (i.e., antiapoptotic) as well as a mitogenic influence (23–25), are increased 48 hr after induction of AP. Pancreatic mRNA levels of the IGF-1R are also elevated during AP. Although the actions of IGF-1 are mediated through binding to the IGF-1R, the increased IGF-1R mRNA levels are probably not due to the increased pancreatic IGF-1 expression since IGF-1 has been shown previously to decrease IGF-1R mRNA levels (41). This finding is consistent with our results since the elevation in IGF-1R precedes the elevation of IGF-1 mRNA levels, which occurs later at 24 to 96 hr when IGF-1R mRNA levels start to decline. Our bax immunostaining findings during AP and the histological appearance of acinar cell apoptosis in cerulein-induced AP support and extend the expression and protein data for cerulein-induced AP.

Initiation of apoptosis can be signaled through different pathways. A current paradigm suggests that cell fate is determined, in part, by the balance between the products of anti- and pro-apoptotic genes of the bcl-2 family of genes (42). The number of genes identified as belonging to the bcl-2 gene family now exceeds 18 (43). The bcl-2 family of genes includes bcl_{XL}, bcl-w, A1/BFL-1, Boo/Diva, Mcl-1, bax, bak, bad, bcl_{XL}s, and others (43). Bcl-2 and bcl_{XL} can inhibit apoptosis; bax can dimerize with bcl-2 or bcl_{XL} and inhibits their function and thereby promotes apoptosis. An increase in the bax/bcl-2 (or bax/bcl_{XL}) ratio fosters apoptosis. In addition, the transcription factor p53 plays a role in the initiation of apoptosis by inducing bax expression (40, 44). In other systems, p53 has been shown to decrease the transcription of the IGF-1R, as well as reduce IGF-1 protein levels and IGF-1R phosphorylation (36, 45). Such activities

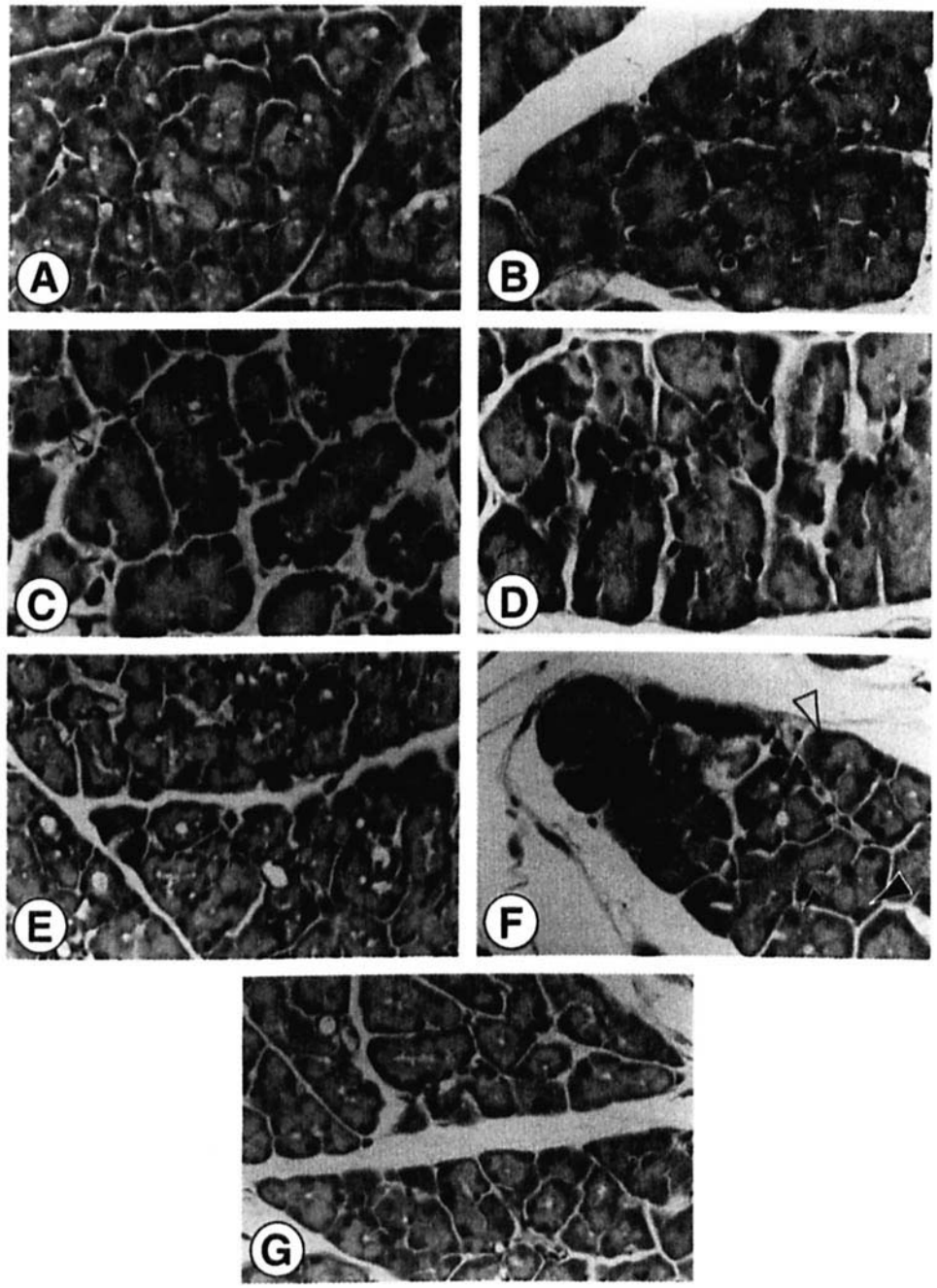

Figure 7. Immunostaining for bax protein in pancreatic acinar cells during AP in mice. Tissue sections are stained with a polyclonal antibody specific for human bax. Counterstaining of nuclei is with hematoxylin. Positive immunostaining for bax in acinar cells is, in general, cytoplasmic. Cytoplasmic with nuclear and nuclear alone bax immunostaining are also observed in acinar cells (×400). (A) In agreement with Western blotting findings, a marginal amount of bax immunostaining is observed in control mice. Bax immunostaining in the cytoplasm and nuclei of pancreatic acini in control mice is identified by the small black and clear arrowheads, respectively. Bax immunostaining (brown hue) is faint. (B) Bax immunostaining in the pancreas 8 hr after induction of AP. Note the widespread (brown hue), cytoplasmic, and nuclear bax immunostaining. (C) Bax immunostaining in the pancreas 12 hr after induction of AP. Note the cytoplasmic and nuclear bax localization. A few positively stained nuclei are identified by the small clear arrowheads. Not all nuclei are stained. (D and E) Bax immunostaining in the pancreas 48 hr after induction of AP. (D) In agreement with our Western blotting findings, note the abundantly strong cytoplasmic and nuclear bax distribution. A few acinar cells with cytoplasmic and nuclear bax immunostaining are identified by the small clear arrowheads. (D and E) Bax immunostaining is also "patchy"; not the entire pancreas is immunostained for bax. (F and G) Bax immunostaining in the pancreas 96 hr after induction of AP. (F) Note the cytoplasmic and nuclear bax localization in acinar cells (small black arrows) in the vicinity of acinar cells with only nuclear staining (large black arrow) or the absence of bax immunostaining (large clear arrow). (G) A region of pancreas with an absence to marginal bax immunostaining 96 hr after induction of AP.

can diminish the antiapoptotic and proliferative actions of IGF-1.

Our results show that AP induces a prompt increase in pancreatic bax mRNA levels. In addition, the elevation in pancreatic levels of bax mRNA is closely followed by an increase in bax protein levels. The peak level of pancreatic bax mRNA levels are achieved 24 hr after induction of AP, whereas peak bax protein in the pancreas occurs 48 hr after

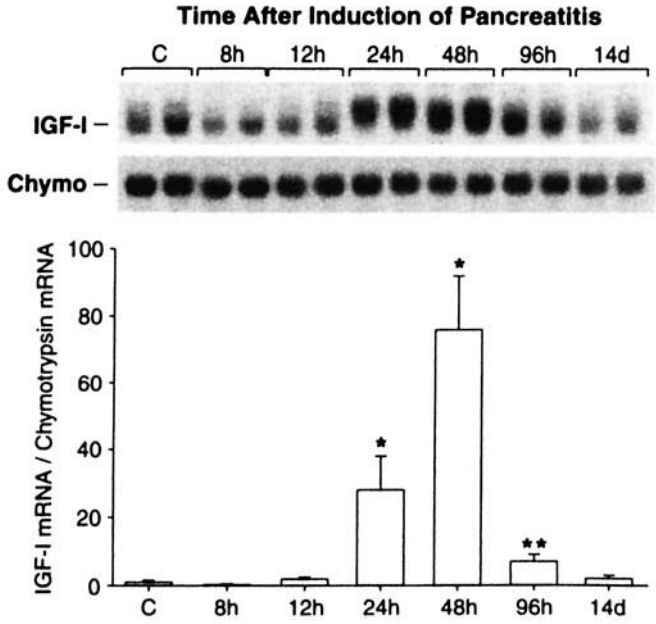

Figure 8. Northern blotting analysis of pancreatic IGF-1 mRNA levels at different times after induction of AP in mice. The three expected IGF-1 transcripts are detected (7.5, 1.7–2.1, and 0.7–1.0), however, only the smaller transcript is shown for ease of presentation. * = $P < 0.005$ versus controls (C); ** = $P < 0.005$ versus controls and earlier groups.

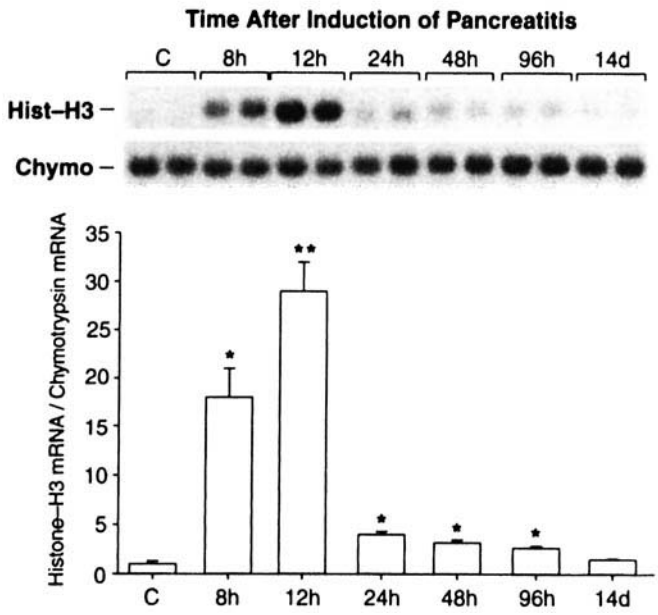

Figure 10. Northern blotting analysis of pancreatic histone H3 mRNA levels at different times after induction of AP in mice. * = $P < 0.005$ versus controls (C); ** = $P < 0.005$ versus controls and earlier groups.

induction of AP. The immunohistochemical localization of bax protein in the acinar cells agrees with and extends our findings, showing an increase in pancreatic mRNA and protein levels during AP. Our bax immunostaining shows abundant cytoplasmic bax protein, as well as nuclear bax localization. Bax has been localized previously to mitochondria, the nuclear membrane, and the endoplasmic reticulum in several tissues (38). The AP-associated elevation in pancreatic bax expression may be signaled partly by p53 since pancreatic p53 mRNA levels are temporally coordinated with those of bax. Together, these findings suggest that acinar cell apoptosis observed during cerulein-induced AP is attributable, at least in part, to the greatly increased bax expression.

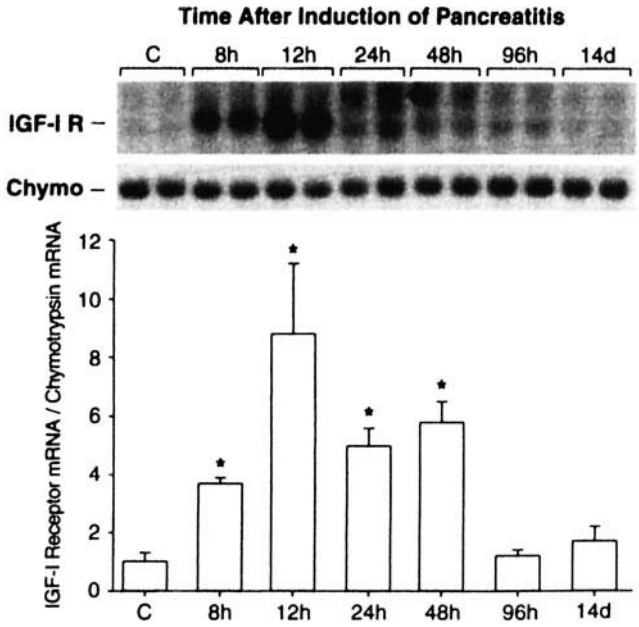

Figure 9. Northern blotting analysis of pancreatic IGF-1R mRNA levels at different times after induction of AP in mice. * = $P < 0.005$ versus controls (C); ** = $P < 0.005$ versus controls and earlier groups.

Our findings also show that pancreatic expression of IGF-1, a cell survival factor and mitogen, is increased in AP. IGF-1 is expressed primarily in the pancreatic ductal epithelium (46) and may act through a paracrine mode. IGF-1 has been shown to prevent induced apoptosis in a variety of cell types (24, 26–28, 30, 31, 47). The increased pancreatic expression of IGF-1 and IGF-1R, especially at the stage that coincides with a transition to recovery and regeneration, may serve to modulate or counteract the apoptotic action of bax and p53 and to promote pancreatic exocrine recovery by acinar cell mitosis. It has been shown in the rat, for example, that pancreatic ^{3}H-thymidine incorporation shows a peak at 1 day and again between 4 and 7 days after induction of AP (7). This earlier study showed that the first peak is localized to intercalated duct cells and interstitial cells, whereas the second peak is localized to remaining acinar cells and reflects pancreatic repair. In the present study, the sustained elevation in pancreatic histone H3 mRNA levels may reflect the protracted phase of acinar cell regeneration that occurs with pancreatic recovery. It is noteworthy that increased pancreatic IGF-1R mRNA levels precedes increased IGF-1 mRNA levels temporally and may serve functionally to insure pancreatic IGF-1 action.

The present study showing induction of apoptotic- and proliferation-related genes during AP extends our understanding of the cellular and molecular events during ceru-

lein-induced AP in mice (7–9, 19, 20). Our laboratory and others have shown histologically that the earliest pancreatic injury (i.e., acinar cell death) occurs within 2 to 3 hr after induction of AP by cerulein, that the maximal injury is observed at 10 to 24 hr after induction of AP, and that the injury is resolved within 96 to 144 hr after induction of AP (9). In the present study we show a dramatic upregulation in the mRNA levels and in one case, protein levels, of proliferative, and of anti- and pro-apoptotic genes. These molecular changes coincide temporally with the documented morphological events in the pancreas and may be mechanisms for activation of acinar cell death by the apoptotic pathway, and pancreatic regeneration during AP. Although we do not demonstrate a strict causative role for these changes in the activation of acinar cell apoptosis and proliferation, they are presumably associated with acinar cell death and pancreatic remodeling during AP.

An earlier *in vitro* study (48) has shown that treatment of a rat acinar cell line, AR4-2J cells, with cerulein induces p53 expression and apoptosis. A recent human study also showed increased p53 expression and apoptotic acinar cell death histology by the terminal transferase-mediated dUTP-biotin nick end labeling reaction (TUNEL) (49). Earlier experimental animal studies have also reported that acinar cells die by apoptosis, as well as by necrosis during AP (10–15). One report indicates that severe forms of AP involve primarily necrosis, whereas mild forms predominantly involve apoptosis and marginal amounts of necrosis of the exocrine pancreas (15). For example, dietary ethionine also causes pancreatic atrophy of the rat pancreas by acinar cell apoptosis (13), and another report indicates that pancreatic duct ligation in the rat resulted primarily in acinar cell apoptosis (10).

Although not addressed in this paper, oxidative stress and the inflammatory process are expected to play a role in human and experimental AP (14, 50–55). During AP in mice, formation of oxygen radicals and their adducts are detected, glutathione levels are decreased, and lipid peroxides are increased. Furthermore, gene products usually associated with oxidative stress are upregulated in the pancreas during experimental AP. Reactive oxygen species can cause DNA damage, resulting in activation of p53 gene expression and apoptotic cell death (40). A recent paper links the activation of the transcription factor, nuclear factor-κB (NF-κB), with the inflammatory and apoptotic responses in cerulein-induced pancreatitis in the rat (56). Although NF-κB is implicated in an antiapoptotic action, NF-κB can also exert a pro-apoptotic action (57–60). In the same paper (56), administration of the antioxidant, *N*-acetylcysteine, blocked NF-κB activation and improved the biomarkers of pancreatitis; however, the percentage of apoptotic acinar cells was unaffected, suggesting that other apoptosis genes participate in the apoptotic process during AP.

In summary, the present findings show that products of several genes involved in the process of cell death by apoptosis are increased during cerulein-induced AP in the mouse. mRNA levels of IGF-1, a potent mitogen and cell-survival factor, and its receptor, IGF-1R, are also increased. These genes may participate in acinar cell apoptosis and proliferation during AP. This is the first report that describes pancreatic mRNA levels and in one case, protein levels of an apoptosis-associated gene and of IGF-1 mRNA levels during cerulein-induced AP. Such information is critical to our understanding and possible devising of approaches to attenuate AP in humans.

1. Banks PA. Medical management of acute pancreatitis and complications. In: Go VW, DiMagno EP, Gardner JD, Lebenthal E, Reber HA, Scheele GA, Eds. The Pancreas: Biology, Pathobiology, and Disease. New York: Raven Press, pp593–611, 1993.
2. Lampel M, Kern HF. Acute interstitial pancreatitis in the rat induced by excessive doses of a pancreatic secretagogue. Virchows Arch A Pathol Pathol Anat **373**:97–117, 1977.
3. Lombardi B, Estes LW, Longnecker DS. Acute hemorrhagic pancreatitis (massive necrosis) with fat necrosis induced in mice by DL-ethionine fed with a choline-deficient diet. Am J Pathol **79**:465–480, 1975.
4. Churg A, Richter WR. Early changes in the exocrine pancreas of the dog and rat after ligation of the pancreatic duct: A light and electron microscopic study. Am J Pathol **63**:521–546, 1971.
5. Gomez G, Townsend CM Jr, Green DW, Rajaraman S, Uchida T, Greeley GH Jr, Soloway RD, Thompson JC. Protective action of luminal bile salts in necrotizing acute pancreatitis in mice. J Clin Invest **86**:323–331, 1990.
6. Ohshio G, Saluja A, Steer ML. Effects of short-term pancreatic duct obstruction in rats. Gastroenterology **100**:196–202, 1991.
7. Elsasser HP, Adler G, Kern HF. Time course and cellular source of pancreatic regeneration following acute pancreatitis in the rat. Pancreas **1**:421–429, 1986.
8. Niederau C, Ferrell LD, Grendell JH. Caerulein-induced acute necrotizing pancreatitis in mice: Protective effects of proglumide, benzotript, and secretin. Gastroenterology **88**:1192–1204, 1985.
9. Niederau C, Niederau M, Luthen R, Strohmeyer G, Ferrell LD, Grendell JH. Pancreatic exocrine secretion in acute experimental pancreatitis. Gastroenterology **99**:1120–1127, 1990.
10. Gukovskaya AS, Perkins P, Zaninovic V, Sandoval D, Rutherford R, Fitzsimmons T, Pandol SJ, Poucell-Hatton S. Mechanisms of cell death after pancreatic duct obstruction in the opossum and the rat. Gastroenterology **110**:875–884, 1996.
11. Kaiser AM, Saluja AK, Lu L, Yamanaka K, Yamaguchi Y, Steer ML. Effects of cycloheximide on pancreatic endonuclease activity, apoptosis, and severity of acute pancreatitis. Am J Physiol **271**:C982–C993, 1996.
12. Doi R, Wada M, Hosotani R, Lee JU, Koshiba T, Fujimoto K, Mori C, Nakamura N, Shiota K, Imamura M. Role of apoptosis in duct obstruction-induced pancreatic involution in rats. Pancreas **14**:39–46, 1997.
13. Walker NI, Winterford CM, Williamson RM, Kerr JF. Ethionine-induced atrophy of rat pancreas involves apoptosis of acinar cells. Pancreas **8**:443–449, 1993.
14. Gukovskaya AS, Gukovsky I, Zaninovic V, Song M, Sandoval D, Gukovsky S, Pandol SJ. Pancreatic acinar cells produce, release, and respond to tumor necrosis factor-α: Role in regulating cell death and pancreatitis. J Clin Invest **100**:1853–1862, 1997.
15. Kaiser AM, Saluja AK, Sengupta A, Saluja M, Steer ML. Relationship between severity, necrosis, and apoptosis in five models of experimental acute pancreatitis. Am J Physiol **269**:C1295–C1304, 1995.
16. Thompson CB. Apoptosis in the pathogenesis and treatment of disease. Science **267**:1456–1462, 1995.
17. Jones BA, Gores GJ. Physiology and pathophysiology of apoptosis in epithelial cells of the liver, pancreas, and intestine. Am J Physiol **273**:G1174–G1188, 1997.

18. Que FG, Gores GJ. Cell death by apoptosis: basic concepts and disease relevance for the gastroenterologist. Gastroenterology **110:**1238–1243, 1996.
19. Adler G, Hupp T, Kern HF. Course and spontaneous regression of acute pancreatitis in the rat. Virchows Arch A Pathol Pathol Anat **382:**31–47, 1979.
20. Fitzgerald PJ, Alvizouri M. Rapid restitution of the rat pancreas following acinar cell necrosis subsequent to ethionine. Nature **170:**929–930, 1952.
21. Buja LM, Eigenbrodt ML, Eigenbrodt EH. Apoptosis and necrosis: Basic types and mechanisms of cell death. Arch Pathol Lab Med **117:**1208–1214, 1993.
22. Chou MY, Chang ALC, Gallagher T, Wong DTW. A rapid method of determine proliferation patterns of normal and malignant tissues by H3 mRNA in situ hybridization. Am J Pathol **136:**729–733, 1990.
23. Baserga R, Prisco M, Hongo A. IGFs and cell growth. In: Rosenfeld RG, Roberts CTJ, Eds. Contemporary Endocrinology: The IGF System. Totowa, NJ: Humana Press, pp329–353, 1999.
24. Geier A, Haimshon M, Beery R, Hemi R, Lunenfeld B. Insulin-like growth factor-1 inhibits cell death induced by cycloheximide in MCF-7 cells: A model system for analyzing control of cell death. *In Vitro* Cell Dev Biol **28A:**725–729, 1992.
25. Kulik G, Klippel A, Weber MJ. Antiapoptotic signalling by the insulin-like growth factor I receptor, phosphatidylinositol 3-kinase, and Akt. Mol Cell Biol **17:**1595–1606, 1997.
26. Galli C, Meucci O, Scorziello A, Werge TM, Calissano P, Schettini G. Apoptosis in cerebellar granule cells is blocked by high KCl, forskolin, and IGF-1 through distinct mechanisms of action: The involvement of intracellular calcium and RNA synthesis. J Neurosci **15:**1172–1179, 1995.
27. Jung Y, Miura M, Yuan J. Suppression of interleukin-1 beta-converting enzyme-mediated cell death by insulin-like growth factor. J Biol Chem **271:**5112–5117, 1996.
28. Chung SY, Billig H, Tilly JL, Furuta I, Tsafriri A, Hsueh AJ. Gonadotropin suppression of apoptosis in cultured preovulatory follicles: Mediatory role of endogenous insulin-like growth factor I. Endocrinology **135:**1845–1853, 1994.
29. Neuenschwander S, Schwartz A, Wood TL, Roberts CT, Jr., Henninghausen L, LeRoith D. Involution of the lactating mammary gland is inhibited by the IGF system in a transgenic mouse model. J Clin Invest **97:**2225–2232, 1996.
30. Resnicoff M, Abraham D, Yutanawiboonchai W, Rotman HL, Kajstura J, Rubin R, Zoltick P, Baserga R. The insulin-like growth factor I receptor protects tumor cells from apoptosis *in vivo*. Cancer Res **55:**2463–2469, 1995.
31. D'Ambrosio C, Valentinis B, Prisco M, Reiss K, Rubini M, Baserga R. Protective effect of the insulin-like growth factor I receptor on apoptosis induced by okadaic acid. Cancer Res **57:**3264–3271, 1997.
32. Oltvai ZN, Milliman CL, Korsmeyer SJ. Bcl-2 heterodimers *in vivo* with a conserved homolog, Bax, that accelerates programmed cell death. Cell **74:**609–619, 1993.
33. Lowe WL Jr, Roberts CT Jr, Lasky SR, LeRoith D. Differential ex pression of alternative 5'-untranslated regions in mRNAs encoding rat insulin-like growth factor I. Proc Natl Acad Sci U S A **84:**8946–8950, 1987.
34. Sato T, Irie S, Krajewski S, Reed JC. Cloning and sequencing of a cDNA encoding the rat Bcl-2 protein. Gene **140:**291–292, 1994.
35. Boise LH, Gonzalez-Garcia M, Postema CE, Ding L, Lindsten T, Turka LA, Mao X, Nunez G, Thompson CB. bcl-x, a bcl-2-related gene that functions as a dominant regulator of apoptotic cell death. Cell Press **74:**597–608, 1993.
36. Werner H, Woloschak M, Adamo M, Shen-Orr Z, Roberts CT Jr, LeRoith D. Developmental regulation of the rat insulin-like growth factor I receptor gene. Proc Natl Acad Sci U S A **86:**7451–7455, 1989.
37. Gross A, McDonnell JM, Korsmeyer SJ. BCL-2 family members and the mitochondria in apoptosis. Genes Dev **13:**1899–1911, 1999.
38. Schendel SL, Montal M, Reed JC. Bcl-2 family proteins as ion-channels. Cell Death Differ **5:**372–380, 1998.
39. Konopleva M, Zhao S, Xie Z, Segall H, Younes A, Claxton DF, Estrov Z, Kornblau SM, Andreeff M. Apoptosis: Molecules and mechanisms. Adv Exp Med Biol **457:**217–236, 1999.
40. Ko LJ, Prives C. p53: puzzle and paradigm. Genes Dev **10:**1054–1072, 1996.
41. Hernandez-Sanchez C, Werner H, Roberts CT Jr, Woo EJ, Hum DW, Rosenthal SM, LeRoith D. Differential regulation of insulin-like growth factor-I (IGF-I) receptor gene expression by IGF-I and basic fibroblastic growth factor. J Biol Chem **272:**4663–4670, 1997.
42. Yang E, Korsmeyer SJ. Molecular thanatopsis: A discourse on the BCL2 family and cell death. Blood **88:**386–401, 1996.
43. Johnson AL. Mcl-1: Just another antiapoptotic Bcl-2 Homolog? Endocrinology **140:**5465–5468, 1999.
44. Miyashita T, Krajewski S, Krajewska M, Wang HG, Lin HK, Liebermann DA, Hoffman B, Reed JC. Tumor suppressor p53 is a regulator of bcl-2 and bax gene expression *in vitro* and *in vivo*. Oncogene **9:**1799–1805, 1994.
45. Ohlsson C, Kley N, Werner H, LeRoith D. p53 regulates insulin-like growth factor-I (IGF-I) receptor expression and IGF-I-induced tyrosine phosphorylation in an osteosarcoma cell line: Interaction between p53 and Sp1. Endocrinology **139:**1101–1107, 1998.
46. Petrik J, Arany E, McDonald TJ, Hill DJ. Apoptosis in the pancreatic islet cells of the neonatal rat is associated with a reduced expression of insulin-like growth factor II that may act as a survival factor. Endocrinology **139:**2994–3004, 1998.
47. Muta K, Krantz SB. Apoptosis of human erythroid colony-forming cells is decreased by stem cell factor and insulin-like growth factor I as well as erythropoietin. J Cell Physiol **156:**264–271, 1993.
48. Sata N, Klonowski-Stumpe H, Han B, Luthen R, Haussinger D, Niederau C. Supraphysiologic concentrations of cerulein induce apoptosis in the rat pancreatic acinar cell line AR4-2J. Pancreas **19:**76–82, 1999.
49. Maacke H, Kessler A, Schmiegel W, Roeder C, Vogel I, Deppert W, Kalthoff H. Overexpression of p53 protein during pancreatitis. Br J Cancer **75:**1501–1504, 1997.
50. Kusske AM, Rongione AJ, Reber HA. Cytokines and acute pancreatitis. Gastroenterology **110:**639–642, 1996.
51. Denham W, Yang J, Fink G, Denham D, Carter G, Ward K, Norman J. Gene targeting demonstrates additive detrimental effects of interleukin 1 and tumor necrosis factor during pancreatitis. Gastroenterology **113:**1741–1746, 1997.
52. Rutledge PL, Saluja AK, Powers RE, Steer ML. Role of oxygen-derived free radicals in diet-induced hemorrhagic pancreatitis in mice. Gastroenterology **93:**41–47, 1987.
53. Fu K, Sarras MP Jr, De Lisle RC, Andrews GK. Expression of oxidative stress-responsive genes and cytokine genes during cerulein-induced acute pancreatitis. Am J Physiol **273:**G696–G705, 1997.
54. Klonowski-Stumpe H, Schreiber R, Grolik M, Schulz HU, Haussinger D, Niederau C. Effect of oxidative stress on cellular functions and cytosolic free calcium of rat pancreatic acinar cells. Am J Physiol **272:**G1489–G1498, 1997.
55. Grady T, Liang P, Ernst SA, Logsdon CD. Chemokine gene expression in rat pancreatic acinar cells is an early event associated with acute pancreatitis. Gastroenterology **113:**1966–1975, 1997.
56. Gukovsky I, Gukovskaya AS, Blinman TA, Zaninovic V, Pandol SJ. Early NF-κb activation is associated with hormone-induced pancreatitis. Am J Physiol **275:**G1402–G1414, 1998.
57. Beg AA, Baltimore D. An essential role for NF-κb in preventing TNF-α-induced cell death. Science **274:**782–784, 1996.
58. Wang CY, Mayo MW, Baldwin AS Jr. TNF-α and cancer therapy-induced apoptosis: Potentiation by inhibition of NF-κb. Science **274:**784–787, 1996.
59. Van Antwerp DJ, Martin SJ, Kafri T, Green DR, Verma IM. Suppression of TNF-α-induced apoptosis by NF-κb. Science **274:**787–789, 1996.
60. Mayo MW, Wang CY, Cogswell PC, Rogers-Graham KS, Lowe SW, Der CJ, Baldwin AS Jr. Requirement of NF-κb activation to suppress p53-independent apoptosis induced by oncogenic Ras. Science **278:**1812–1815, 1997.